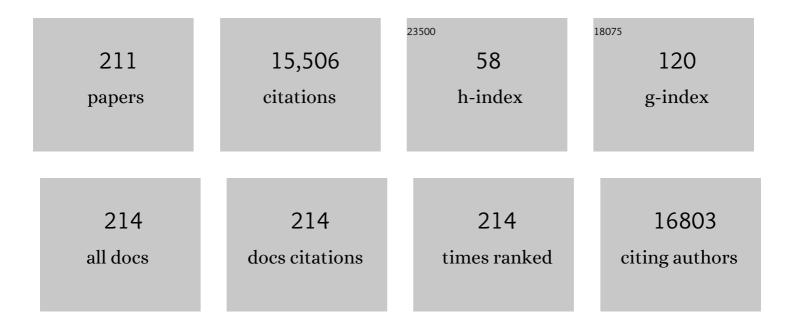
## Eray S Aydil

## List of Publications by Year in descending order

Source: https://exaly.com/author-pdf/6404418/publications.pdf Version: 2024-02-01



#	Article	IF	CITATIONS
1	Growth of Oriented Single-Crystalline Rutile TiO <sub>2</sub> Nanorods on Transparent Conducting Substrates for Dye-Sensitized Solar Cells. Journal of the American Chemical Society, 2009, 131, 3985-3990.	6.6	2,243
2	Nanowire-based dye-sensitized solar cells. Applied Physics Letters, 2005, 86, 053114.	1.5	969
3	Photosensitization of ZnO Nanowires with CdSe Quantum Dots for Photovoltaic Devices. Nano Letters, 2007, 7, 1793-1798.	4.5	935
4	Hot-Electron Transfer from Semiconductor Nanocrystals. Science, 2010, 328, 1543-1547.	6.0	775
5	Polyethylene glycol-coated biocompatible surfaces. Journal of Biomedical Materials Research Part B, 2000, 51, 343-351.	3.0	535
6	Synthesis and characterization of ZnO nanowires and their integration into dye-sensitized solar cells. Nanotechnology, 2006, 17, S304-S312.	1.3	408
7	Mechanism of hydrogen-induced crystallization of amorphous silicon. Nature, 2002, 418, 62-65.	13.7	379
8	Dye-sensitized solar cells based on semiconductor morphologies with ZnO nanowires. Solar Energy Materials and Solar Cells, 2006, 90, 607-622.	3.0	344
9	Nonthermal Plasma Synthesis of Nanocrystals: Fundamental Principles, Materials, and Applications. Chemical Reviews, 2016, 116, 11061-11127.	23.0	309
10	Doping high-surface-area mesoporous TiO <sub>2</sub> microspheres with carbonate for visible light hydrogen production. Energy and Environmental Science, 2014, 7, 2592.	15.6	253
11	Solar Cells Based on Junctions between Colloidal PbSe Nanocrystals and Thin ZnO Films. ACS Nano, 2009, 3, 3638-3648.	7.3	250
12	Imaging and phase identification of Cu2ZnSnS4 thin films using confocal Raman spectroscopy. Journal of Vacuum Science and Technology A: Vacuum, Surfaces and Films, 2011, 29, .	0.9	231
13	Photovoltaic manufacturing: Present status, future prospects, and research needs. Journal of Vacuum Science and Technology A: Vacuum, Surfaces and Films, 2011, 29, .	0.9	226
14	Calculation of the lattice dynamics and Raman spectra of copper zinc tin chalcogenides and comparison to experiments. Journal of Applied Physics, 2012, 111, .	1.1	221
15	Size control and quantum confinement in Cu2ZnSnS4 nanocrystals. Chemical Communications, 2011, 47, 11721.	2.2	219
16	Stable Ordering in Langmuir-Blodgett Films. Science, 2001, 293, 1292-1295.	6.0	200
17	TiO <sub>2</sub> –B/Anatase Core–Shell Heterojunction Nanowires for Photocatalysis. ACS Applied Materials & Interfaces, 2011, 3, 4444-4450.	4.0	162
18	Oriented single crystalline titanium dioxide nanowires. Nanotechnology, 2008, 19, 505604.	1.3	138

#	Article	IF	CITATIONS
19	Modeling of the sheath and the energy distribution of ions bombarding rf-biased substrates in high density plasma reactors and comparison to experimental measurements. Journal of Applied Physics, 1999, 86, 4799-4812.	1.1	127
20	Alkali-metal-enhanced grain growth in Cu <sub>2</sub> ZnSnS <sub>4</sub> thin films. Energy and Environmental Science, 2014, 7, 1931-1938.	15.6	124
21	Silicon hydride composition of plasma-deposited hydrogenated amorphous and nanocrystalline silicon films and surfaces. Journal of Vacuum Science and Technology A: Vacuum, Surfaces and Films, 1998, 16, 3199-3210.	0.9	121
22	Investigation of SiO2 plasma enhanced chemical vapor deposition through tetraethoxysilane using attenuated total reflection Fourier transform infrared spectroscopy. Journal of Vacuum Science and Technology A: Vacuum, Surfaces and Films, 1995, 13, 2355-2367.	0.9	117
23	Growth mechanism and characterization of zinc oxide hexagonal columns. Applied Physics Letters, 2003, 83, 3797-3799.	1.5	114
24	Electron transport and recombination in polycrystalline TiO2 nanowire dye-sensitized solar cells. Applied Physics Letters, 2007, 91, 123116.	1.5	112
25	Strong Electronic Coupling in Two-Dimensional Assemblies of Colloidal PbSe Quantum Dots. ACS Nano, 2009, 3, 1532-1538.	7.3	109
26	Effect of chamber wall conditions on Cl and Cl2 concentrations in an inductively coupled plasma reactor. Journal of Vacuum Science and Technology A: Vacuum, Surfaces and Films, 2002, 20, 43-52.	0.9	107
27	Valence Band Alignment at Cadmium Selenide Quantum Dot and Zinc Oxide (101ì0) Interfaces. Journal of Physical Chemistry C, 2008, 112, 8419-8423.	1.5	102
28	Study of surface reactions during plasma enhanced chemical vapor deposition of SiO2 from SiH4, O2, and Ar plasma. Journal of Vacuum Science and Technology A: Vacuum, Surfaces and Films, 1996, 14, 2062-2070.	0.9	96
29	Modeling of SiO2 deposition in high density plasma reactors and comparisons of model predictions with experimental measurements. Journal of Vacuum Science and Technology A: Vacuum, Surfaces and Films, 1998, 16, 544-563.	0.9	96
30	Heteroepitaxial growth of Cu2O thin film on ZnO by metal organic chemical vapor deposition. Journal of Crystal Growth, 2009, 311, 4188-4192.	0.7	96
31	Growth mechanism of titanium dioxide nanowires for dye-sensitized solar cells. Nanotechnology, 2008, 19, 095604.	1.3	94
32	Electron transport and recombination in dye-sensitized solar cells made from single-crystal rutile TiO2 nanowires. Physical Chemistry Chemical Physics, 2009, 11, 9648.	1.3	92
33	Nanowire-quantum-dot solar cells and the influence of nanowire length on the charge collection efficiency. Applied Physics Letters, 2009, 95, .	1.5	92
34	Epitaxial growth of ZnO nanowires on a- and c-plane sapphire. Journal of Crystal Growth, 2005, 274, 407-411.	0.7	91
35	Compact floating ion energy analyzer for measuring energy distributions of ions bombarding radio-frequency biased electrode surfaces. Review of Scientific Instruments, 1999, 70, 2689-2698.	0.6	89
36	On the growth mechanism of a-Si:H. Thin Solid Films, 2001, 383, 154-160.	0.8	89

#	Article	IF	CITATIONS
37	Luminescence from plasma deposited silicon films. Journal of Applied Physics, 1997, 81, 2410-2417.	1.1	88
38	Plasma-induced crystallization of silicon nanoparticles. Journal Physics D: Applied Physics, 2014, 47, 075202.	1.3	83
39	Effect of H2 addition on surface reactions during CF4/H2 plasma etching of silicon and silicon dioxide films. Journal of Vacuum Science and Technology A: Vacuum, Surfaces and Films, 1997, 15, 2508-2517.	0.9	79
40	Energy distribution of ions bombarding biased electrodes in high density plasma reactors. Journal of Vacuum Science and Technology A: Vacuum, Surfaces and Films, 1999, 17, 506-516.	0.9	79
41	Etching of high aspect ratio structures in Si using SF[sub 6]/O[sub 2] plasma. Journal of Vacuum Science and Technology A: Vacuum, Surfaces and Films, 2004, 22, 606.	0.9	79
42	High electron mobility in thin films formed via supersonic impact deposition of nanocrystals synthesized in nonthermal plasmas. Nature Communications, 2014, 5, 5822.	5.8	77
43	Lowâ€ŧemperature plasma enhanced chemical vapor deposition of SiO2. Applied Physics Letters, 1994, 65, 3185-3187.	1.5	74
44	Maintaining reproducible plasma reactor wall conditions: SF6 plasma cleaning of films deposited on chamber walls during Cl2/O2 plasma etching of Si. Journal of Vacuum Science and Technology A: Vacuum, Surfaces and Films, 2002, 20, 1195-1201.	0.9	73
45	First principles calculation of the electronic properties and lattice dynamics of Cu2ZnSn(S1â^'xSex)4. Journal of Applied Physics, 2012, 111, .	1.1	73
46	Influence of Atmospheric Gases on the Electrical Properties of PbSe Quantum-Dot Films. Journal of Physical Chemistry C, 2010, 114, 9988-9996.	1.5	72
47	Reasons for lower dielectric constant of fluorinated SiO2 films. Journal of Applied Physics, 1998, 83, 2172-2178.	1.1	70
48	Absolute densities of N and excited N2 in a N2 plasma. Applied Physics Letters, 2003, 83, 4918-4920.	1.5	70
49	Low temperature plasma deposition of silicon nitride from silane and nitrogen plasmas. Journal of Vacuum Science and Technology A: Vacuum, Surfaces and Films, 1998, 16, 2794-2803.	0.9	66
50	Anatase TiO2 films with reactive {001} facets on transparent conductive substrate. Chemical Communications, 2011, 47, 9507.	2.2	66
51	Microstructure Evolution and Crystal Growth in Cu <sub>2</sub> ZnSnS <sub>4</sub> Thin Films Formed By Annealing Colloidal Nanocrystal Coatings. Chemistry of Materials, 2014, 26, 3191-3201.	3.2	66
52	Effect of hydrogen on catalyst nanoparticles in carbon nanotube growth. Journal of Applied Physics, 2010, 108, .	1.1	65
53	Atomistic simulation study of the interactions of SiH3 radicals with silicon surfaces. Journal of Applied Physics, 1999, 86, 2872-2888.	1.1	63
54	Structure and chemical composition of fluorinated SiO2 films deposited using SiF4/O2 plasmas. Journal of Vacuum Science and Technology A: Vacuum, Surfaces and Films, 1997, 15, 2893-2904.	0.9	62

#	Article	IF	CITATIONS
55	Abstraction of hydrogen by SiH3 from hydrogen-terminated Si(001)-(2×1) surfaces. Surface Science, 1998, 418, L8-L13.	0.8	62
56	Nonequilibrium-Plasma-Synthesized ZnO Nanocrystals with Plasmon Resonance Tunable via Al Doping and Quantum Confinement. Nano Letters, 2015, 15, 8162-8169.	4.5	62
57	Computational Study of Structural and Electronic Properties of Lead-Free CsMI <sub>3</sub> Perovskites (M = Ge, Sn, Pb, Mg, Ca, Sr, and Ba). Journal of Physical Chemistry C, 2018, 122, 7838-7848.	1.5	62
58	Interactions of SiH radicals with silicon surfaces: An atomic-scale simulation study. Journal of Applied Physics, 1998, 84, 3895-3911.	1.1	60
59	Transport Limited Growth of Zinc Oxide Nanowires. Crystal Growth and Design, 2009, 9, 2783-2789.	1.4	58
60	Investigation of low temperature SiO2 plasma enhanced chemical vapor deposition. Journal of Vacuum Science & Technology an Official Journal of the American Vacuum Society B, Microelectronics Processing and Phenomena, 1996, 14, 738.	1.6	57
61	Crossover From Nanoscopic Intergranular Hopping to Conventional Charge Transport in Pyrite Thin Films. ACS Nano, 2013, 7, 2781-2789.	7.3	57
62	Measurement of absolute radical densities in a plasma using modulated-beam line-of-sight threshold ionization mass spectrometry. Journal of Vacuum Science and Technology A: Vacuum, Surfaces and Films, 2004, 22, 71-81.	0.9	55
63	Rapid facile synthesis of Cu <sub>2</sub> ZnSnS <sub>4</sub> nanocrystals. Journal of Materials Chemistry A, 2014, 2, 10389-10395.	5.2	53
64	Surface hydride composition of plasma deposited hydrogenated amorphous silicon: in situ infrared study of ion flux and temperature dependence. Surface Science, 2003, 530, 1-16.	0.8	50
65	New diagnostic method for monitoring plasma reactor walls: Multiple total internal reflection Fourier transform infrared surface probe. Review of Scientific Instruments, 2001, 72, 3260-3269.	0.6	49
66	Self-Regulation of Cu/Sn Ratio in the Synthesis of Cu <sub>2</sub> ZnSnS <sub>4</sub> Films. Chemistry of Materials, 2015, 27, 2507-2514.	3.2	49
67	Evolution of structure, morphology, and reactivity of hydrogenated amorphous silicon film surfaces grown by molecular-dynamics simulation. Applied Physics Letters, 2001, 78, 2685-2687.	1.5	47
68	Abstraction of atomic hydrogen by atomic deuterium from an amorphous hydrogenated silicon surface. Journal of Chemical Physics, 2002, 117, 10805-10816.	1.2	47
69	Orientation and Morphological Evolution of Catalyst Nanoparticles During Carbon Nanotube Growth. ACS Nano, 2010, 4, 5087-5094.	7.3	47
70	Visible luminescence from nanocrystalline silicon films produced by plasma enhanced chemical vapor deposition. Applied Physics Letters, 1996, 68, 1415-1417.	1.5	46
71	Deposition of silicon oxychloride films on chamber walls during Cl2/O2 plasma etching of Si. Journal of Vacuum Science and Technology A: Vacuum, Surfaces and Films, 2002, 20, 499-506.	0.9	46
72	Infrared detection of hydrogen-generated free carriers in polycrystalline ZnO thin films. Journal of Applied Physics, 2005, 97, 043522.	1.1	45

#	Article	IF	CITATIONS
73	Phase Stability and Stoichiometry in Thin Film Iron Pyrite: Impact on Electronic Transport Properties. ACS Applied Materials & Interfaces, 2015, 7, 14130-14139.	4.0	45
74	Multiple steady states in electron cyclotron resonance plasma reactors. Journal of Vacuum Science and Technology A: Vacuum, Surfaces and Films, 1993, 11, 2883-2892.	0.9	44
75	Langmuir probe measurements of electron energy probability functions in dusty plasmas. Journal Physics D: Applied Physics, 2015, 48, 105204.	1.3	44
76	Realâ€Time, In Situ Monitoring of Roomâ€Temperature Silicon Surface Cleaning Using Hydrogen and Ammonia Plasmas. Journal of the Electrochemical Society, 1993, 140, 3316-3321.	1.3	43
77	An analysis of temperature dependent current–voltage characteristics of Cu2O–ZnO heterojunction solar cells. Thin Solid Films, 2011, 519, 6613-6619.	0.8	43
78	Synthesis of single-crystalline anatase nanorods and nanoflakes on transparent conducting substrates. Chemical Communications, 2012, 48, 8565.	2.2	42
79	Ammonia plasma passivation of GaAs in downstream microwave and radio-frequency parallel plate plasma reactors. Journal of Vacuum Science & Technology an Official Journal of the American Vacuum Society B, Microelectronics Processing and Phenomena, 1993, 11, 195.	1.6	41
80	Feature-scale model of Si etching in SF6 plasma and comparison with experiments. Journal of Vacuum Science and Technology A: Vacuum, Surfaces and Films, 2005, 23, 99-113.	0.9	41
81	Effects of Chamber Wall Conditions on Cl Concentration and Si Etch Rate Uniformity in Plasma Etching Reactors. Journal of the Electrochemical Society, 2003, 150, G418.	1.3	38
82	Hydrogen-induced crystallization of amorphous silicon thin films. I. Simulation and analysis of film postgrowth treatment with H2 plasmas. Journal of Applied Physics, 2006, 100, 053514.	1.1	38
83	Electron Dynamics at the ZnO (101Ì0) Surface. Journal of Physical Chemistry C, 2008, 112, 14682-14692.	1.5	38
84	Synthesis of Cu <sub>2</sub> (Zn <sub>1â^'x</sub> Co <sub>x</sub> )SnS <sub>4</sub> nanocrystals and formation of polycrystalline thin films from their aqueous dispersions. Journal of Materials Chemistry A, 2018, 6, 999-1008.	5.2	36
85	Modeling of Plasma Etching Reactors Including Wafer Heating Effects. Journal of the Electrochemical Society, 1993, 140, 1471-1481.	1.3	35
86	Structure and Composition of Zn <sub><i>x</i></sub> Cd <sub>1–<i>x</i></sub> S Films Synthesized through Chemical Bath Deposition. ACS Applied Materials & Interfaces, 2012, 4, 3676-3684.	4.0	35
87	Sputter deposition of semicrystalline tin dioxide films. Thin Solid Films, 2012, 520, 2554-2561.	0.8	35
88	Lead-free double perovskites Cs <sub>2</sub> InCuCl <sub>6</sub> and (CH <sub>3</sub> NH <sub>3</sub> ) <sub>2</sub> InCuCl <sub>6</sub> : electronic, optical, and electrical properties. Nanoscale, 2019, 11, 11173-11182.	2.8	35
89	Transport Evidence for Sulfur Vacancies as the Origin of Unintentional n-Type Doping in Pyrite FeS <sub>2</sub> . ACS Applied Materials & Interfaces, 2019, 11, 15552-15563.	4.0	35
90	Formation of Stable Metal Halide Perovskite/Perovskite Heterojunctions. ACS Energy Letters, 2020, 5, 3443-3451.	8.8	35

#	Article	IF	CITATIONS
91	Oriented single-crystalline TiO <sub>2</sub> nanowires on titanium foil for lithium ion batteries. Journal of Materials Research, 2010, 25, 1588-1594.	1.2	34
92	Requirements for plasma synthesis of nanocrystals at atmospheric pressures. Journal Physics D: Applied Physics, 2015, 48, 035205.	1.3	34
93	Resolving the discrepancies in the reported optical absorption of low-dimensional non-toxic perovskites, Cs <sub>3</sub> Bi <sub>2</sub> Br <sub>9</sub> and Cs <sub>3</sub> BiBr <sub>6</sub> . Journal of Materials Chemistry C, 2020, 8, 10456-10463.	2.7	34
94	Theoretical and Experimental Investigations of Chlorine RF Glow Discharges: I . Theoretical. Journal of the Electrochemical Society, 1992, 139, 1396-1406.	1.3	33
95	Mechanism and energetics of dissociative adsorption of SiH3 on the hydrogen-terminated Si(001)-(2×1) surface. Chemical Physics Letters, 2000, 329, 304-310.	1.2	33
96	Feature-scale model of Si etching in SF6â^•O2 plasma and comparison with experiments. Journal of Vacuum Science and Technology A: Vacuum, Surfaces and Films, 2005, 23, 1430-1439.	0.9	33
97	Microstructure Evolution During Selenization of Cu <sub>2</sub> ZnSnS <sub>4</sub> Colloidal Nanocrystal Coatings. Chemistry of Materials, 2016, 28, 1266-1276.	3.2	33
98	Relation between the ion flux, gas phase composition, and wall conditions in chlorine plasma etching of silicon. Journal of Vacuum Science and Technology A: Vacuum, Surfaces and Films, 2003, 21, 589-595.	0.9	32
99	Detection of combinative infrared absorption bands in thin silicon dioxide films. Applied Physics Letters, 1997, 70, 3269-3271.	1.5	31
100	Theoretical study of the interactions of SiH2 radicals with silicon surfaces. Journal of Applied Physics, 1999, 86, 5497-5508.	1.1	31
101	In situprobing of surface hydrides on hydrogenated amorphous silicon using attenuated total reflection infrared spectroscopy. Journal of Vacuum Science and Technology A: Vacuum, Surfaces and Films, 2002, 20, 781-789.	0.9	31
102	Effect of Nanocrystal Size and Carbon on Grain Growth during Annealing of Copper Zinc Tin Sulfide Nanocrystal Coatings. Chemistry of Materials, 2017, 29, 1676-1683.	3.2	31
103	Functionalization of Cadmium Selenide Quantum Dots with Poly(ethylene glycol): Ligand Exchange, Surface Coverage, and Dispersion Stability. Langmuir, 2017, 33, 8239-8245.	1.6	31
104	ZnO Nanocrystal Networks Near the Insulator–Metal Transition: Tuning Contact Radius and Electron Density with Intense Pulsed Light. Nano Letters, 2017, 17, 4634-4642.	4.5	30
105	Hydrogen-induced crystallization of amorphous Si thin films. II. Mechanisms and energetics of hydrogen insertion into Si–Si bonds. Journal of Applied Physics, 2006, 100, 053515.	1.1	29
106	Getting Moore from Solar Cells. Science, 2012, 338, 625-626.	6.0	28
107	Cu2ZnSnS4 nanocrystal dispersions in polar liquids. Chemical Communications, 2013, 49, 3549.	2.2	28
108	Mechanism and activation energy barrier for H abstraction by H(D) from a-Si:H surfaces. Surface Science, 2002, 515, L469-L474.	0.8	27

#	Article	IF	CITATIONS
109	Improving the damp-heat stability of copper indium gallium diselenide solar cells with a semicrystalline tin dioxide overlayer. Solar Energy Materials and Solar Cells, 2012, 101, 270-276.	3.0	27
110	Formation of Copper Zinc Tin Sulfide Thin Films from Colloidal Nanocrystal Dispersions via Aerosol-Jet Printing and Compaction. ACS Applied Materials & Interfaces, 2015, 7, 11526-11535.	4.0	27
111	Selective removal of Cu <sub>2â^`x</sub> (S,Se) phases from Cu <sub>2</sub> ZnSn(S,Se) <sub>4</sub> thin films. Green Chemistry, 2016, 18, 5814-5821.	4.6	27
112	Potential resolution to the doping puzzle in iron pyrite: Carrier type determination by Hall effect and thermopower. Physical Review Materials, 2017, 1, .	0.9	27
113	Surface conduction in <mml:math xmlns:mml="http://www.w3.org/1998/Math/MathML"&gt; <mml:mi>n</mml:mi>-type pyrite<mml:math xmlns:mml="http://www.w3.org/1998/Math/MathML"&gt; <mml:msub><mml:mi>FeS</mml:mi><mml:mn>2<td>0.9 in&gt; <td>27 msub&gt; </td></td></mml:mn></mml:msub></mml:math </mml:math 	0.9 in> <td>27 msub&gt; </td>	27 msub>
114	Chystals. Physical Review Materials, 2017, 1, . Theoretical and Experimental Investigations of Chlorine RF Glow Discharges: II . Experimental. Journal of the Electrochemical Society, 1992, 139, 1406-1412.	1.3	26
115	Incidence angle distributions of ions bombarding grounded surfaces in high density plasma reactors. Materials Science in Semiconductor Processing, 1998, 1, 75-82.	1.9	26
116	Atomistic calculation of the SiH3 surface reactivity during plasma deposition of amorphous silicon thin films. Surface Science, 2004, 572, L339-L347.	0.8	26
117	Metal-oxide broken-gap tunnel junction for copper indium gallium diselenide tandem solar cells. Solar Energy Materials and Solar Cells, 2015, 133, 133-142.	3.0	26
118	Real-time monitoring of surface chemistry during plasma processing. Pure and Applied Chemistry, 1994, 66, 1381-1388.	0.9	25
119	Plasma and surface diagnostics during plasma-enhanced chemical vapor deposition of SiO2 from SiH4/O2/Ar discharges. Thin Solid Films, 1996, 290-291, 427-434.	0.8	24
120	Surface Smoothening Mechanism of Amorphous Silicon Thin Films. Physical Review Letters, 2005, 95, 216102.	2.9	24
121	Catalyst rotation, twisting, and bending during multiwall carbon nanotube growth. Carbon, 2010, 48, 3840-3845.	5.4	23
122	Hydrogen etching and cutting of multiwall carbon nanotubes. Journal of Vacuum Science and Technology B:Nanotechnology and Microelectronics, 2010, 28, 1187-1194.	0.6	23
123	Effects of Water Adsorption and Surface Oxidation on the Electrical Conductivity of Silicon Nanocrystal Films. Journal of Physical Chemistry C, 2013, 117, 4211-4218.	1.5	23
124	Realâ€ŧime,insitumonitoring of surface reactions during plasma passivation of GaAs. Applied Physics Letters, 1993, 62, 3156-3158.	1.5	22
125	Deposition of nanocrystalline silicon films at room temperature. Journal of Applied Physics, 2007, 102, 043305.	1.1	22
126	Multiple steady states in a radio frequency chlorine glow discharge. Journal of Applied Physics, 1991, 69, 109-114.	1.1	21

#	Article	IF	CITATIONS
127	Electron cyclotron resonance plasma reactor for cryogenic etching. Review of Scientific Instruments, 1993, 64, 3572-3584.	0.6	21
128	Angle-dependent photoluminescence spectra of hydrogenated amorphous silicon thin films. Applied Physics Letters, 2000, 77, 3346-3348.	1.5	21
129	Growth and characterization of hydrogenated amorphous silicon thin films from SiH2 radical precursor: Atomic-scale analysis. Journal of Applied Physics, 2004, 95, 1792-1805.	1.1	21
130	Feature scale model of Si etching in SF6â^•O2â^•HBr plasma and comparison with experiments. Journal of Vacuum Science and Technology A: Vacuum, Surfaces and Films, 2006, 24, 350-361.	0.9	21
131	Nonthermal plasma synthesis of metal sulfide nanocrystals from metalorganic vapor and elemental sulfur. Journal Physics D: Applied Physics, 2015, 48, 314004.	1.3	21
132	Controlling Cu <sub>2</sub> ZnSnS <sub>4</sub> (CZTS) phase in microwave solvothermal synthesis. Journal of Materials Chemistry A, 2017, 5, 23179-23189.	5.2	21
133	Sulfur Vacancy Clustering and Its Impact on Electronic Properties in Pyrite FeS <sub>2</sub> . Chemistry of Materials, 2020, 32, 4820-4831.	3.2	21
134	Hydrogen in Si–Si bond center and platelet-like defect configurations in amorphous hydrogenated silicon. Journal of Vacuum Science & Technology an Official Journal of the American Vacuum Society B, Microelectronics Processing and Phenomena, 2004, 22, 2719.	1.6	20
135	Interaction of SiH3 radicals with deuterated (hydrogenated) amorphous silicon surfaces. Surface Science, 2005, 598, 35-44.	0.8	20
136	Metallorganic Chemical Vapor Deposition of ZnO Nanowires from Zinc Acetylacetonate and Oxygen. Journal of the Electrochemical Society, 2009, 156, H52.	1.3	20
137	Real time in situ monitoring of surfaces during glow discharge processing: NH3 and H2 plasma passivation of GaAs. Journal of Vacuum Science & Technology an Official Journal of the American Vacuum Society B, Microelectronics Processing and Phenomena, 1995, 13, 258.	1.6	19
138	Atomistic simulation of SiH interactions with silicon surfaces during deposition from silane containing plasmas. Applied Physics Letters, 1998, 72, 578-580.	1.5	19
139	Mechanisms and energetics of SiH3 adsorption on the pristine Si(001)-(2×1) surface. Chemical Physics Letters, 2001, 344, 249-255.	1.2	19
140	Structural and electrical properties of Cu2O thin films deposited on ZnO by metal organic chemical vapor deposition. Journal of Vacuum Science and Technology A: Vacuum, Surfaces and Films, 2010, 28, 1338-1343.	0.9	19
141	Origin of Intraband Optical Transitions in Ag <sub>2</sub> Se Colloidal Quantum Dots. Journal of Physical Chemistry C, 2021, 125, 17556-17564.	1.5	19
142	Modeling of Heat Transport and Wafer Heating Effects during Plasma Etching. Journal of the Electrochemical Society, 1996, 143, 3674-3680.	1.3	18
143	Analysis of diamond nanocrystal formation from multiwalled carbon nanotubes. Physical Review B, 2009, 80, .	1.1	18
144	Plasma synthesis of stoichiometric Cu2S nanocrystals stabilized by oleylamine. Chemical Communications, 2014, 50, 8346.	2.2	18

#	Article	IF	CITATIONS
145	Observation of an Internal p–n Junction in Pyrite FeS <sub>2</sub> Single Crystals: Potential Origin of the Low Open Circuit Voltage in Pyrite Solar Cells. , 2020, 2, 861-868.		18
146	In Situ Probing and Atomistic Simulation of a-Si:H Plasma Deposition. Materials Research Society Symposia Proceedings, 2001, 664, 111.	0.1	17
147	Effect of H2 dilution on the surface composition of plasma-deposited silicon films from SiH4. Applied Surface Science, 1998, 133, 148-151.	3.1	16
148	Temperature dependence of precursor–surface interactions in plasma deposition of silicon thin films. Chemical Physics Letters, 2005, 414, 61-65.	1.2	16
149	Reactive sputter deposition of pyrite structure transition metal disulfide thin films: Microstructure, transport, and magnetism. Journal of Applied Physics, 2012, 112, .	1.1	16
150	Metal-insulator transition in a semiconductor nanocrystal network. Science Advances, 2019, 5, eaaw1462.	4.7	16
151	Formation and removal of composite halogenated silicon oxide and fluorocarbon films deposited on chamber walls during plasma etching of multiple film stacks. Journal of Vacuum Science & Technology an Official Journal of the American Vacuum Society B, Microelectronics Processing and Phenomena, 2002. 20. 1939.	1.6	15
152	Structure optimization for a high efficiency CIGS solar cell. , 2010, , .		15
153	Silanol Concentration Depth Profiling during Plasma Deposition of SiO2 Using Multiple Internal Reflection Infrared Spectroscopy. Journal of the Electrochemical Society, 1997, 144, 3963-3967.	1.3	14
154	Excited-State Dynamics in CZTS Nanocrystals. Journal of Physical Chemistry Letters, 2013, 4, 2711-2714.	2.1	14
155	Synthesis of Cu2ZnSnS4 thin films directly onto conductive substrates via selective thermolysis using microwave energy. Chemical Communications, 2014, 50, 5902.	2.2	14
156	An on-wafer probe array for measuring two-dimensional ion flux distributions in plasma reactors. Review of Scientific Instruments, 2002, 73, 3494-3499.	0.6	13
157	Etching of high aspect ratio features in Si using SF6â^•O2â^•HBr and SF6â^•O2â^•Cl2 plasma. Journal of Vacuum Science and Technology A: Vacuum, Surfaces and Films, 2005, 23, 1592-1597.	0.9	13
158	Sputtered metal oxide broken gap junctions for tandem solar cells. Solar Energy Materials and Solar Cells, 2015, 132, 515-522.	3.0	13
159	Intense pulsed light annealing of copper zinc tin sulfide nanocrystal coatings. Journal of Vacuum Science and Technology A: Vacuum, Surfaces and Films, 2016, 34, 051204.	0.9	13
160	Efficient near-infrared emission from lead-free ytterbium-doped cesium bismuth halide perovskites. Journal of Materials Chemistry A, 2021, 9, 13026-13035.	5.2	13
161	High photoluminescence quantum yield near-infrared emission from a lead-free ytterbium-doped double perovskite. Materials Horizons, 0, , .	6.4	13
162	Control of an unstable electron cyclotron resonance plasma. Applied Physics Letters, 1993, 62, 2039-2041.	1.5	12

#	Article	IF	CITATIONS
163	Atomic-scale analysis of deposition and characterization ofa-Si:H thin films grown from SiH radical precursor. Journal of Applied Physics, 2002, 92, 842-852.	1.1	12
164	Copper–Zinc–Tin–Sulfide Thin Films via Annealing of Ultrasonic Spray Deposited Nanocrystal Coatings. ACS Applied Materials & Interfaces, 2017, 9, 18865-18871.	4.0	12
165	Carrier-gas assisted vapor deposition for highly tunable morphology of halide perovskite thin films. Sustainable Energy and Fuels, 2019, 3, 2447-2455.	2.5	12
166	Atomic-scale analysis of fundamental mechanisms of surface valley filling during plasma deposition of amorphous silicon thin films. Surface Science, 2005, 574, 123-143.	0.8	11
167	In situmeasurement of the ion incidence angle dependence of the ion-enhanced etching yield in plasma reactors. Journal of Vacuum Science and Technology A: Vacuum, Surfaces and Films, 2006, 24, 2176-2186.	0.9	11
168	First-principles theoretical analysis of pure and hydrogenated crystalline carbon phases and nanostructures. Chemical Physics Letters, 2009, 474, 168-174.	1.2	11
169	Plasmonic Interactions through Chemical Bonds of Surface Ligands on PbSe Nanocrystals. Chemistry of Materials, 2014, 26, 3328-3333.	3.2	11
170	Molecular dynamics study of the interactions of small thermal and energetic silicon clusters with crystalline and amorphous silicon surfaces. Journal of Vacuum Science & Technology an Official Journal of the American Vacuum Society B, Microelectronics Processing and Phenomena, 2001, 19, 634.	1.6	9
171	Visualizing the evolution of surface bond straining during radical-surface interactions in plasma deposition processes. IEEE Transactions on Plasma Science, 2002, 30, 112-113.	0.6	9
172	Collision of a long DNA molecule with an isolated nanowire. Electrophoresis, 2010, 31, 3675-3680.	1.3	9
173	Variable range hopping conduction in ZnO nanocrystal thin films. Nanotechnology, 2018, 29, 415202.	1.3	9
174	Machine learning enhanced spectroscopic analysis: towards autonomous chemical mixture characterization for rapid process optimization. , 2022, 1, 35-44.		9
175	Abstraction of hydrogen by SiH radicals from hydrogenated amorphous silicon surfaces. Surface Science, 2000, 459, L475-L481.	0.8	8
176	Spatial and temporal variation of ion flux in the presence of an instability in inductively coupled SF6plasmas. Plasma Sources Science and Technology, 2003, 12, 148-151.	1.3	8
177	Layered mesoporous nanostructures for enhanced light harvesting in dye-sensitized solar cells. Journal of Renewable and Sustainable Energy, 2011, 3, 043106.	0.8	8
178	Atmospheric-pressure glow plasma synthesis of plasmonic and photoluminescent zinc oxide nanocrystals. Journal of Applied Physics, 2016, 119, 243302.	1.1	8
179	Vapor deposition of CsPbBr3 thin films by evaporation of CsBr and PbBr2. Journal of Vacuum Science and Technology A: Vacuum, Surfaces and Films, 2021, 39, .	0.9	8
180	Quantum confinement in few layer SnS nanosheets. Nanotechnology, 2019, 30, 245705.	1.3	7

#	Article	IF	CITATIONS
181	Quantitative Understanding of Superparamagnetic Blocking in Thoroughly Characterized Ni Nanoparticle Assemblies. Chemistry of Materials, 2020, 32, 6494-6506.	3.2	7
182	Visualizing radical-surface interactions in plasma deposition processes: reactivity of SiH/sub 3/ radicals with Si surfaces. IEEE Transactions on Plasma Science, 1999, 27, 104-105.	0.6	6
183	Two-dimensional ion flux distributions in inductively coupled plasmas: Effect of adding electronegative gases to Ar. Journal of Applied Physics, 2002, 92, 6444-6450.	1.1	6
184	Mechanism and energetics of dimerization of SiH2 radicals on H-terminated Si()-(2×1) surfaces. Surface Science, 2003, 540, L623-L630.	0.8	6
185	Experimental and theoretical study of two-dimensional ion flux uniformity at the wafer plane in inductively coupled plasmas. IEEE Transactions on Plasma Science, 2003, 31, 614-627.	0.6	6
186	Substrate and temperature dependence of the formation of the Earth abundant solar absorber Cu2ZnSnS4 by ex situ sulfidation of cosputtered Cu-Zn-Sn films. Journal of Vacuum Science and Technology A: Vacuum, Surfaces and Films, 2014, 32, 061203.	0.9	5
187	Spatial and temporal variation of the ion flux impinging on the wafer surface in presence of a plasma instability. IEEE Transactions on Plasma Science, 2002, 30, 120-121.	0.6	4
188	Tin dioxide as an alternative window layer for improving the damp-heat stability of copper indium gallium diselenide solar cells. Journal of Vacuum Science and Technology A: Vacuum, Surfaces and Films, 2012, 30, .	0.9	4
189	Plasmonic nanocomposites of zinc oxide and titanium nitride. Journal of Vacuum Science and Technology A: Vacuum, Surfaces and Films, 2020, 38, 042404.	0.9	4
190	Mitigation of the internal <i>p-n</i> junction in <mml:math xmlns:mml="http://www.w3.org/1998/Math/MathML"&gt;<mml:mrow><mml:msub><mml:mi>CoS</mml:mi><mm -contacted <mml:math xmlns:mml="http://www.w3.org/1998/Math/MathML"&gt;<mml:mrow><mml:msub><mml:mi>FeS</mml:mi><mml single crystals: Accessing bulk semiconducting transport. Physical Review Materials, 2021, 5, .</mml </mml:msub></mml:mrow></mml:math </mm </mml:msub></mml:mrow></mml:math 	0.9	4
191	Thermal transport in ZnO nanocrystal networks synthesized by nonthermal plasma. Physical Review Materials, 2020, 4, .	0.9	4
192	Carbon Diffusion from Methane into Walls of Carbon Nanotube through Structurally and Compositionally Modified Iron Catalyst. Microscopy and Microanalysis, 2011, 17, 582-586.	0.2	3
193	Physical vapor deposition of the halide perovskite CsBi2Br7. Journal of Vacuum Science and Technology A: Vacuum, Surfaces and Films, 2021, 39, .	0.9	3
194	Atomic-Scale Analysis of the Reactivity of Radicals from Silane/Hydrogen Plasmas with Silicon Surfaces. Materials Research Society Symposia Proceedings, 1997, 485, 107.	0.1	2
195	Growth and Characterization of ZnO Nanowires. Materials Research Society Symposia Proceedings, 2003, 776, 791.	0.1	2
196	Chemically Induced Magnetic Dead Shells in Superparamagnetic Ni Nanoparticles Deduced from Polarized Small-Angle Neutron Scattering. ACS Applied Materials & Interfaces, 2022, 14, 33491-33504.	4.0	2
197	Atomic-Scale Analysis of Plasma-Enhanced Chemical Vapor Deposition from SiH4/2 Plasmas on Si Substrates. Materials Research Society Symposia Proceedings, 1998, 507, 673.	0.1	1
198	Incorporation of Cl into Hydrogenated Amorphous Silicon without Optical Band Gap Widening. Japanese Journal of Applied Physics, 2002, 41, L1357-L1359.	0.8	1

#	Article	IF	CITATIONS
199	Surface Processes during Growth of Hydrogenated Amorphous Silicon. Materials Research Society Symposia Proceedings, 2004, 808, 311.	0.1	1
200	Visualizing the evolution of surface morphology and surface bond strain during plasma deposition of amorphous silicon thin films. IEEE Transactions on Plasma Science, 2005, 33, 228-229.	0.6	1
201	Sulfurization studies of the potential thin film solar absorber Cu <inf>2</inf> ZnSnS <inf>4</inf> . , 2010, , .		1
202	Wide band-gap Culn <inf>1−X</inf> Ga <inf>X</inf> Se <inf>2</inf> based chalcopyrite absorbers for tandem cell applications. , 2011, , .		1
203	Challenges in deposition of wide band gap copper indium aluminum gallium selenide (CIACS) thin films for tandem solar cells. , 2014, , .		1
204	Preface for the AVS Peter Mark award 40th anniversary collection. Journal of Vacuum Science and Technology A: Vacuum, Surfaces and Films, 2021, 39, 031601.	0.9	1
205	Reaction Control in Amorphous Silicon Film Deposition by Hydrogen Chloride. Materials Research Society Symposia Proceedings, 2003, 762, 1521.	0.1	0
206	The Role of SiH3 Diffusion in Determining the Surface Smoothness of Plasma-Deposited Amorphous Si Thin Films: An Atomic-Scale Analysis. Materials Research Society Symposia Proceedings, 2005, 862, 321.	0.1	0
207	Efficient continuous-flow chemical bath deposition of CdS films as buffer layers for chalcogenide-based solar cells. , 2013, , .		0
208	Sixty years of diversity. Journal of Vacuum Science and Technology A: Vacuum, Surfaces and Films, 2013, 31, 050401.	0.9	0
209	Preface for the Special Topic Collection Commemorating the Career of John Coburn. Journal of Vacuum Science and Technology A: Vacuum, Surfaces and Films, 2020, 38, .	0.9	0
210	Preface for the Festschrift Honoring Dr. Steve Rossnagel. Journal of Vacuum Science and Technology A: Vacuum, Surfaces and Films, 2020, 38, .	0.9	0
211	Plasma diagnostics and modeling of lithium-containing plasmas. Journal Physics D: Applied Physics, 2022, 55, 254001.	1.3	0